Chemical Science

ROYAL SOCIETY OF CHEMISTRY

EDGE ARTICLE

View Article Online
View Journal

Cite this: DOI: 10.1039/d6sc00279j

All publication charges for this article have been paid for by the Royal Society of Chemistry

Electrochemically cooperative halogen-cation delivery enables modular electrophilic haloesterification of both activated and unactivated alkenes

He-Huan Xu, *[a] Duo-Duo Qian,[a] Yi Fan,*[bc] Jia-Jia Zhang,[a] Chang-Le Guo[a] and Hai-Chao Xu *[b]

Intermolecular haloesterification of alkenes is a practical platform for modular ester synthesis. However, current methods are restricted to aryl-activated and directing-group-containing alkenes, leaving low-reactivity, electron-deficient alkenes with alkyl substituents largely underexplored. Notably, electrophilic reactions involving chloroesterification of electron-deficient alkenes are also challenging due to the difficulty in controlling selectivity. In this work, we present an electrochemically cooperative halogen-cation delivery strategy that achieves modular electrophilic haloesterification of both activated and unactivated alkenes with good chemo-, regio-, and diastereoselectivity levels. It exhibits enhanced reactivity (with yields of up to 90%) and selectivity (regioselectivities and diastereoselectivities exceeding 20 : 1), as the amide mediates the transfer of Cl^+ to the alkene, enabling the formation of stable halogen-containing cationic intermediates (β-halo carbocation or halonium) in the electrochemically oxidative 'electrophile–nucleophile' ('E–Nu') approach. Di-, tri-, and tetrasubstituted alkenes displaying various electronic properties, as well as terminal alkenes, have been successfully haloesterified, showcasing the good tolerance of the strategy to the presence of functional groups. Moreover, the strategy is applicable to gram-scale synthesis and late-stage elaboration of bioactive compounds. It also enables the construction of quaternary carbons, even multiple contiguous ones, in reactions.

Received 12th January 2026
Accepted 13th March 2026

DOI: 10.1039/d6sc00279j

rsc.li/chemical-science

Alkene halofunctionalization enables the simultaneous formation of anti-selective vicinal carbon-halo and carbon-heteroatom bonds.[1–7] Haloesterification reactions employ simple, readily available alkenes instead of traditional alcohol nucleophiles to react with carboxylic variants, producing versatile halogenated ester derivatives, providing a facile and practical synthetic tool for diversifying and modularizing the synthesis of esters, especially challenging ones exhibiting high steric hindrance.[8,9] Intermolecular reactions, which provide clearer operational advantages for modular haloesterification have garnered increasing attention compared with intramolecular haloesterification, which requires the preparation of alkenoic acid substrates.

Intermolecular haloesterification of unactivated alkenes, aryl-activated alkenes, and those containing a directing group has been well established using the typical 'electrophile–nucleophile' ('E–Nu') strategy,[10–21] nucleophile–nucleophile ('Nu–Nu') strategy,[22,23] and radical-polar crossover approach.[24,25] However, alkyl-substituted, electron-deficient alkenes remain significantly underdeveloped due to their low halonium affinity and weak electrophilicity. In particular, electrophilic reactions involving chloroesterification of electron-deficient alkenes are more challenging due to the difficulty in controlling selectivity.[26,27] Therefore, innovative strategies are urgently needed to achieve modular haloesterification of both activated and unactivated alkenes, particularly sterically hindered variants (Scheme 1a).

As an alternative, a technique involving oxidative 'E–Nu' driven by consecutive paired electrolysis[28–34] can generate highly active X_2 to promote shuttle reactions through sequential oxidation and reduction of an electronically neutral halogenated molecule.[35–40] It can eliminate interference from other nucleophilic ions and allow the generation rate of active species to be precisely controlled by adjusting the electric current or voltage, thereby offering a direct and highly efficient strategy for achieving haloesterification. Because the reactivity and selectivity of the technique can be strongly modulated by factors such as electronegativity and bonding flexibility of halogen

[a]Henan Key Laboratory of Organic Functional Molecule and Drug Innovation, School of Chemistry and Chemical Engineering, Henan Normal University, Xinxiang 53007, China. E-mail: hehuanxu@htu.edu.cn

[b]State Key Laboratory of Physical Chemistry of Solid Surfaces, College of Chemistry and Chemical Engineering, Xiamen University, Xiamen 361005, China. E-mail: fanyi1019@xmu.edu.cn; haichao.xu@xmu.edu.cn

[c]College of Materials Science and Engineering, Huaqiao University, Xiamen, 361021, China

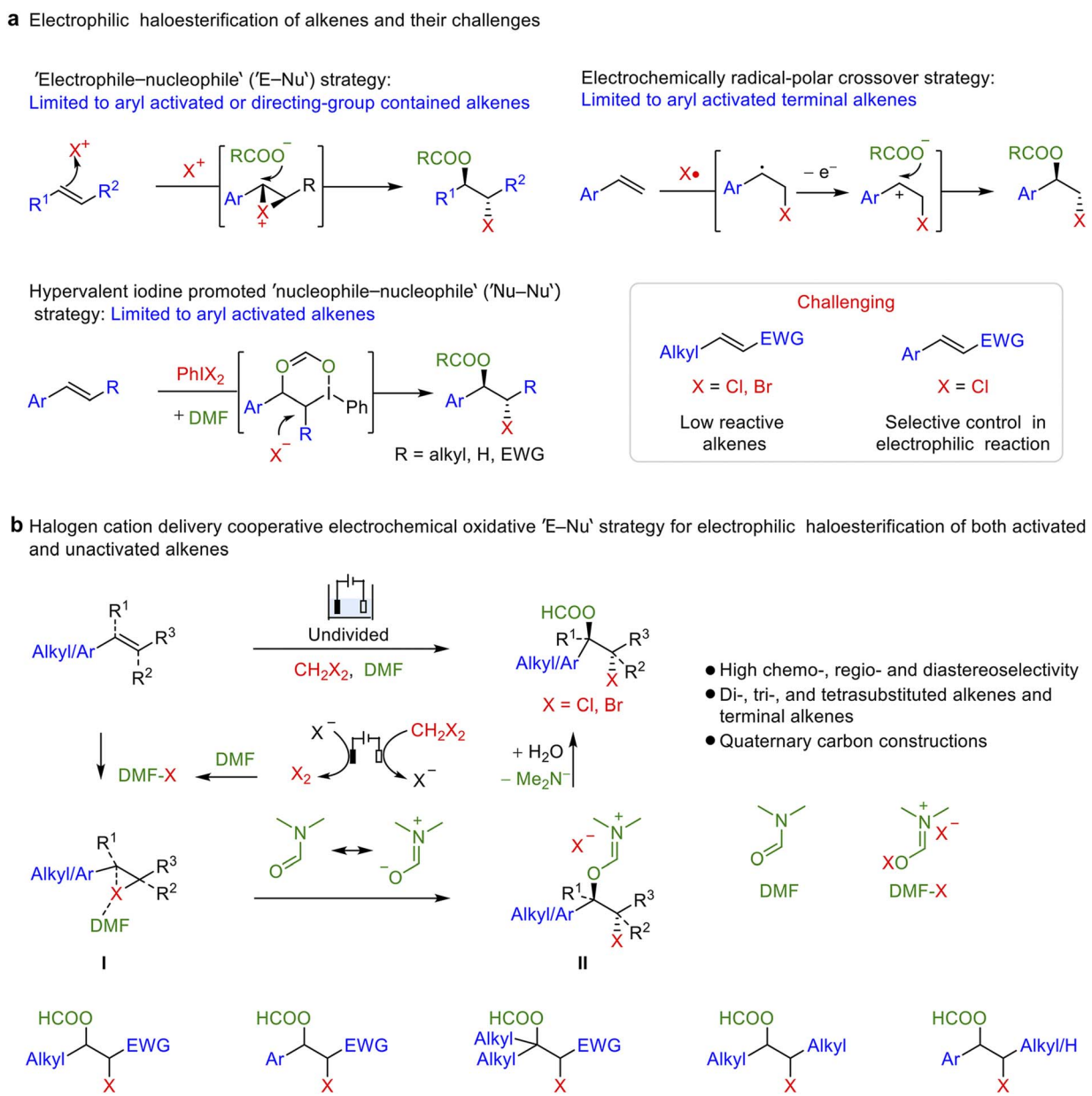

Scheme 1 Challenges and our strategy for the haloesterification of both activated and unactivated alkenes. (a) Electrophilic haloesterification of alkenes and its challenges. (b) Halogen-cation delivery design: electrochemical 'electrophile–nucleophile' ('E–Nu') strategy for electrophilic haloesterification of both activated and unactivated alkenes. Ar, aryl; EWG, electron-withdrawing group.

cations,[41] the choice of appropriate delivery reagent for halogen cations, as we propose here, is crucial for promoting reactivity and enhancing the selectivity of heterodifunctionalization in both activated and unactivated internal alkenes.

Herein, we report an electrochemically oxidative 'E–Nu' strategy combined with halogen-cation delivery for achieving modular electrophilic haloesterification of alkenes with good chemo-, regio-, and diastereoselectivities (Scheme 1b). It deploys an electrochemically driven shuttle reaction coupled with amide-mediated transfer of halogen cations to activate the real-time generation of X_2, and subsequently forms amide-X to promote the formation of β-halocarbocation or halonium, which is then subjected to nucleophilic attack by an acyl transfer reagent in an anti-addition manner. Both activated and unactivated di-, tri-, and tetrasubstituted alkenes, as well as terminal alkenes, are compatible. Excellent reactivity and selectivity are also observed in the construction of quaternary carbons, including multiple contiguous ones, in reactions of tri- and tetrasubstituted alkenes.

Results and discussions

Reaction condition optimization

3-Phenylpropyl 3-methylbut-2-enoate **1** was used as the model substrate to optimize the reaction conditions through direct electrolysis in an undivided cell with a two-electrode system

Table 1 Optimization of reaction conditions[a]

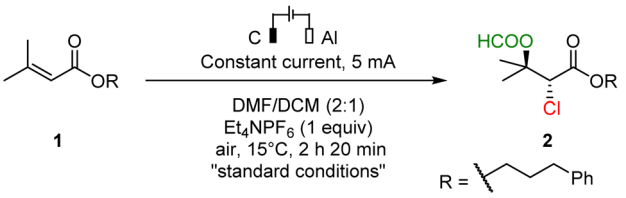

Entry	Deviation from standard conditions	Yield [%][b]
1	None	90[c]
2	No DCM	NR
3	No DMF	NR
4	$CHCl_3$, DCE instead of DCM	73[c], 46 (22)
5	NCS (1.5 or 2.0 equiv) instead of DCM without electrolysis	N.R, N.R.
6	DMF/DCM = 1 : 2, 3 : 1	72[c], 59[c]
7	Reaction at 6 V	0[c] (100)
8	Reaction at 9 V	40[c] (60)
9	Reaction at 12 V	77[c]
10	Reaction at 3 mA, 10 mA	90[c], 36[c] (61)
11	Reaction at 30 °C	72[c]
12	Reaction at 80 °C	38[c] (58)
13	Reaction at 100 °C	20[c] (80)
14	nBu$_4$NPF$_6$, Me$_4$NPF$_6$, Et$_4$NBF$_4$ as electrolyte	75[c], 29[c] (36), 83[c]
15	Copper plate (1 cm × 1 cm) as cathode	60[c]
16	Foam nickel (1 cm × 1 cm) as cathode	34[c] (34)
17	Carbon rod (Φ 0.6 cm) as cathode	77[c]

[a] Reaction conditions: carbon rod anode (Φ 0.6 cm × 10 cm), aluminum plate cathode (1.0 cm × 2.5 cm), **1** alkene (0.1 mmol), solvent (6 mL), air, 2 h 20 min. [b] Yield of the major diastereomer determined from ^{1}H NMR analysis with 1,3,5-trimethoxybenzene as the internal standard. [c] Isolated yield, unreacted 1 in brackets. DMF, *N*,*N*-dimethyl formyl amide; DCM, dichloromethane; DCE, 1,2-dichloroethane; NR, no reaction; NCS, *N*-chlorosuccinimide.

(Table 1). The optimal conditions for the desired chloroformyloxylation product **2** (90% yield, entry 1) involved electrolysis at 15 °C, employing a carbon rod anode, an aluminum plate cathode, and a constant current of 5 mA, with Et_4NPF_6 as the electrolyte in a mixed solvent (DMF/DCM = 2 : 1, v/v) under air. DCM and DMF were essential for the reaction; without them, no reaction occurred (entries 2 and 3). But the reaction did proceed when replacing DCM with $CHCl_3$ or DCE (entry 4), with DCM, $CHCl_3$ and DCE potentially serving as sources of chlorine. But when the traditional Cl^+ donor NCS was used as the halogen source, no reaction was observed without electrolysis (entry 5). A similar phenomenon was observed with NBS as the halogen source (Tables S1 and S2). The DMF/DCM ratio was also crucial for achieving a good yield (entry 6). We speculated that DMF not only acted as a synthon in the reaction but also as a halogen cation deliverer. Constant voltage was found to be disadvantageous for the transformation, as evidenced by the detection of alkene **1** reduction and dichlorination byproducts (entries 7–9). Moreover, elevated current accelerated the transformation but did not improve the yield (entry 10), attributed to the formation of olefin halogenation by-products. Elevated temperatures, however, clearly decreased the efficiency of the transformation (entries 11–13) and the diastereoselectivity (Table S3), attributed to their accelerating the reversible decomposition of the halonium intermediates, and leading to elimination of HCl from the product during the process. When the electrolyte was changed to nBu$_4$NBF$_4$, Me$_4$NPF$_6$, or Et$_4$NBF$_4$, reduced yet still acceptable yields were obtained (entry 14). Additionally, other cathode materials such as copper plates, foam nickel, and carbon rods were tested, but they yielded lower conversion to product than did the aluminum plate (entries 15–17). The aluminum plate was concluded to effectively suppress the reduction of both the alkene (Fig. S4) and DMF, while providing a suitable reduction rate for CH_2Cl_2 (where, $r_{Ni} > r_{Cu} > r_C > r_{Al}$) (Fig. S5). These by-products were clearly observed when copper plates or foam nickel were used as the cathode.

Evaluation of the scope of alkyl-substituted alkenes

The optimal conditions were initially applied to the haloesterification of di-, tri- and tetra-alkyl-substituted substrates (Scheme 2). These reactions have the potential to form important quaternary carbons, including continuous multiple quaternary carbons. Fourteen types of trisubstituted alkenes were systematically examined. 2-Cyclobutylidene acetates, 3,3-dimethyl acrylates, 3-methyl-5-phenyl pent-2-enoate, and 3-methyl-3-aryl acrylates were shown to be suitable substrates for delivering chloroformyloxylation products with a quaternary carbon at the 3-position (**3–6**). β-Carbocation rearrangement byproducts were detected during the isolation of **5** and **6**. In contrast, the 3,3-diphenylsubstituted structure yielded only

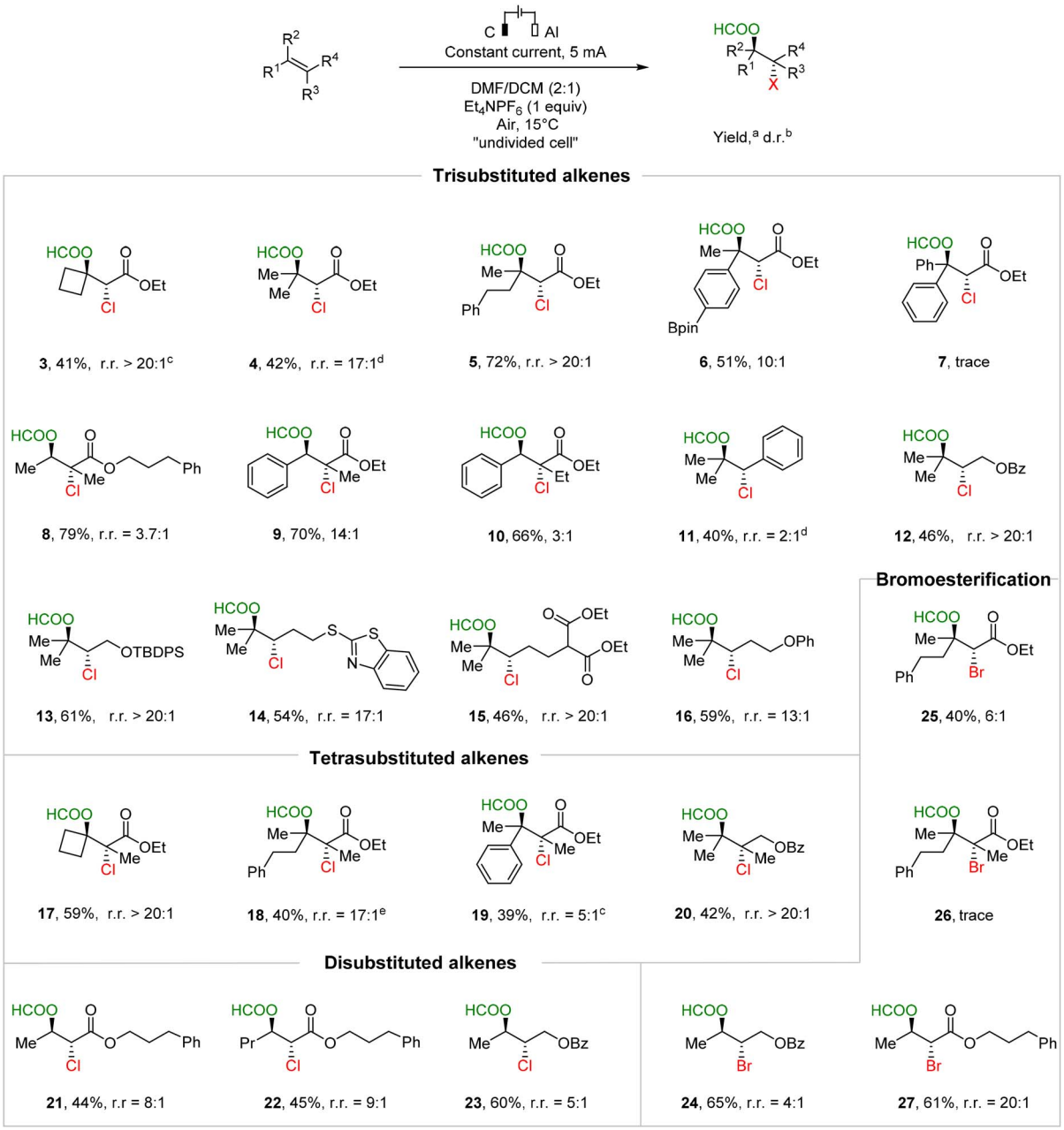

Scheme 2 Reaction scope of alkyl-substituted alkenes. Reaction conditions: Table 1, entry 1. Conditions: alkene (0.1 mmol), DMF (4 mL), CH_2X_2 (2 mL). 1–8 h (0.93–7.46 F). (a) Isolated yield of the major diastereoisomer. (b) Determined from ^{1}H NMR analysis of the crude reaction mixture. (c) Reaction at RT. (d) Reaction at 5 °C. (e) Reaction with Me_4NBF_4. Bz, benzoxyl; TBDPS, *tert*-butyldiphenysilyl; d.r., diastereomeric ratio; r.r., regioisomeric ratio.

trace amounts of the product (**7**)—due to the instability of the diphenyl cationic intermediate, which led to the production of β-H elimination byproducts. The introduction of 2-methyl-3-methyl acrylate achieved a quaternary carbon product at the 2-position in 79% yield with 3.7 : 1 regioselectivity (**8**), likely due to the low charge separation at the 2-position. 2-Methyl-3-phenylacrylate gave the corresponding product in 70% yield with a 14 : 1 diastereoselectivity (**9**); 2-ethyl-3-phenylacrylate gave products in a similar (66%) yield—but with considerably lower diastereoselectivity (3 : 1), due to the greater steric hindrance at the 2-position (**10**). (2-Methylprop-1-en-1-yl) benzene led to the desired products in moderate yields but with low regioselectivity (2 : 1) (**11**). Notably, neutral trisubstituted alkenes bearing functional groups such as OBz, TBDPS, 2-thio benzothiazole, diethyl 2-malonate, and phenoxyl successfully furnished the corresponding products in moderate to good yields (46% to 61%) and high regioselectivities (most >20 : 1) (**12–16**). The cases of obtaining only moderate yields were attributed to β-carbocation rearrangement, dihalogenation, and the low boiling point of the product.

Subsequently, a series of tetra-alkyl-substituted alkenes were rigorously assessed under standard conditions or under otherwise identical conditions, along with the replacement of Et_4NPF_6 with Me_4NBF_4, where β-carbocation rearrangement and dihalogenation byproducts or the low boiling point of the product were the major causes of having moderate yields. We were delighted to discover that 2-cyclobutylidene propanoate, 2-methyl-3-phenyl but-2-enoate, 2,3-dimethyl but-2-enoate, and 2,3-dimethyl-5-phenyl pent-2-enoate were all well tolerated. The haloesterification products having two quaternary carbons were obtained in moderate yields (39% to 59%) and good regioselectivities (up to >20 : 1) (**17–19**). As expected, neutral tetrasubstituted alkenes were well accommodated, providing the desired products in yields of 42% with high regioselectivities (>20 : 1) (**20**). Low-reactivity 3-alkyl-substituted *E*-acrylates were also tolerated (**21**, **22**) by prolonging the reaction time to 6 h. When unactivated 1,2-disubstituted neutral alkenes were tested, the corresponding products were obtained in 60% yield and a 4 : 1 regioselectivity (**23**). More importantly, the strategy proved applicable to the bromoesterification of di-,trisubstituted alkenes (**24**, **25**, **27**). However, alkenes displaying higher steric hindrance were found to be incompatible with this reaction. For example, in the case of a tetrasubstituted alkene, the bromoesterification product was obtained only in trace amounts (<5%) (**26**).

Evaluation of the scope of aryl-activated alkenes

Encouraged by the success of the strategy that facilitated the haloesterification of alkyl-substituted substrates, we set out to investigate its ability to achieve electrophilic haloesterification of aryl-activated electron-withdrawing alkenes and other disubstituted and terminal alkenes (Scheme 3). Reactions of a series of ethyl *E*-3-aryl acrylates, substituted at different positions on the phenyl ring and having diverse electronic properties, proceeded efficiently; they afforded the desired chloroformyloxylation products with yields ranging from 46% to 85% and diastereoselectivities of up to 20 : 1 (**28–43**). Functional groups such as F, Cl, Br, CO_2Me, Bpin, and even a heteroaromatic ring, imidazole, were well tolerated. These results were suggestive of the position of substitution on the phenyl ring having minimal impact on both the yield and diastereocontrol. Importantly, the strategy could be scaled up to the gram level, achieving a 60% yield. However, substrates bearing electron-withdrawing groups showed reduced reactivity levels, requiring longer reaction times to get good yields. In some cases, unreacted alkene was still detected when the substrate contained a strongly electron-withdrawing *p*-COOMe-group on the phenyl ring (**34**), owing to the lower halonium affinity of these alkenes. Substrates with 3,5- or 3,4-disubstituents on the phenyl ring (**44–47**), as well as a bulkier substrate having 2,4,6-trisubstituents (**48**), were also successfully converted into highly decorated chloroformyloxylation products by extending the reaction time to 4–7 h. Fused (hetero) aromatic rings such as 2-naphthalene, 6-quinoxaline, and benzofuran were compatible, with yields from 34% to 62% and diastereoselectivities of up to >20 : 1 (**49–51**).

With novel functionalization required, we applied the strategy to the late-stage synthetic elaboration of complex, biologically relevant scaffolds and drug molecules, including steroid-based core structures and estrone-based core structures (**52**, **53**). In addition to the ethyl ester, other *E*-disubstituted alkenes—such as methyl ester, isopropyl ester, phenyl ketone, and Weinreb amide at the 2-position—proved compatible for furnishing the desired chloroformyloxylation products (**54–57**). No product was detected when the substrate contained strongly electron-withdrawing CN or NO_2 groups (**58**, **59**), and oxidative decomposition occurred for prolonged reaction times. Notably, when *E*-β-methyl styrene was introduced, the chloroformyloxylation product was obtained in a 58% yield and an 8 : 1 diastereoselectivity (**60**). Similarly, 1*H*-indene and 1,2-dihydronaphthalene were also compatible substrates, affording the desired benzo ring products (**61**, **62**). Surprisingly, *Z*-β-methyl styrene proved to be compatible, delivering a satisfactory yield of 65% with a 5 : 1 diastereoselectivity (**60′**). The method was also suitable for styrene, achieving a 60% yield (**63**). However, 1-phenyl 1-alkyl alkenes (**64**) gave mixtures of chloroformyloxylation products and β-carbocation rearrangement byproducts, while 1,1-diphenyl alkenes (**65**) gave only HCl-elimination byproducts. Overall, 1-phenyl 2-alkyl alkenes and neutral alkenes were more reactive than electron-withdrawing ones. Furthermore, this strategy enabled the successful bromoesterification of activated and unactivated alkenes, including 3-aryl acrylates (**66**), 1*H*-indene (**67**) and 1,2-dihydronaphthalene (**68**). More importantly, it can also be effectively applied to chloroacetates (**69**, **70**) and chlorination of aromatics, such as products containing substituted indoles (**71**), benzothiophene (**72**), and pyrazole (**73**).

To sum up, the halogen-cation-delivery-promoted electrochemically oxidative 'electrophile–nucleophile' ('E–Nu') approach successfully achieved chemo-, regio-, and diastereoselective electrophilic haloesterification of both activated and unactivated alkenes. A wide range of alkenes, including di-, tri-, and tetrasubstituted alkenes, as well as terminal alkenes, were found to be compatible. Excellent reactivity and selectivity were also observed in the construction of quaternary carbons, including multiple contiguous ones, in reactions of tri- and tetrasubstituted alkenes. However, alkenes with strongly electron-withdrawing substituents (*e.g.*, CN, NO_2) showed poor reactivity. Highly sterically hindered alkenes were incompatible with the bromoesterification reaction; for example, in the case of tetrasubstituted alkenes, the corresponding product was obtained only in trace amounts.

Mechanistic studies

Rationally designed experiments were conducted to investigate the reaction mechanism associated with this electrochemical haloesterification of alkenes. Results of radical-trap experiments showed that the use of the radical inhibitor O_2 slightly reduced the yield of product **29** compared to N_2 (Scheme 4a), suggestive of the reaction proceeding *via* an ionic mechanism. This mechanism was further supported by Hammett plot experiments,[42] which gave a ρ value of −0.9, indicating

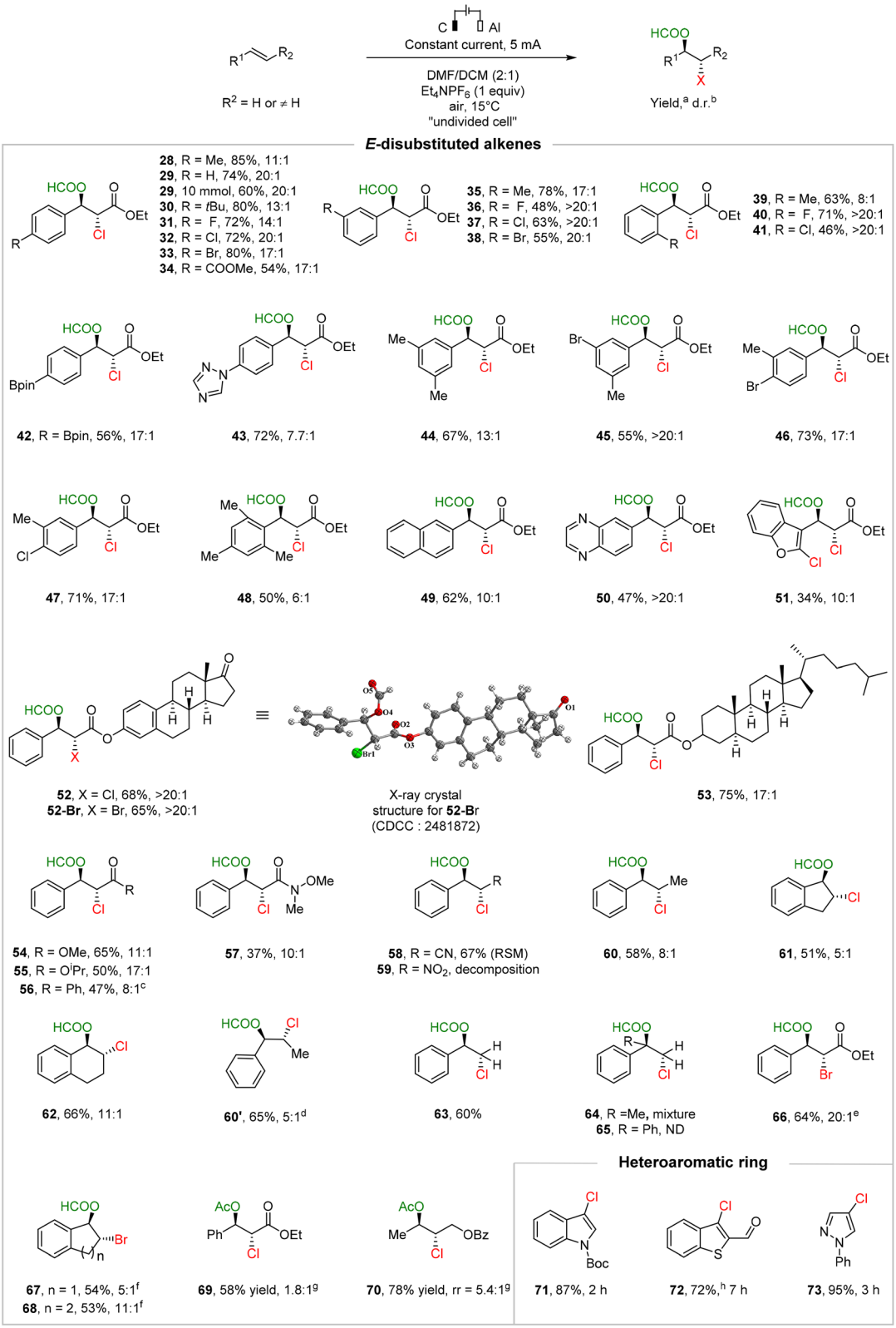

Scheme 3 Reaction scope of aryl-activated disubstituted alkenes and terminal alkenes. Conditions: alkene (0.1 mmol), DMF (4 mL), CH_2X_2 (2 mL). 2–13 h (1.87–12.12 F). (a) Isolated yield of major diastereoisomer. (b) Determined from ^{1}H NMR analysis of the crude reaction mixture. (c) Reaction at RT. (d) Reaction at 5 °C. (e) Reaction in DMF/CH_2Br_2 (3.75 mL/1.25 mL). (f) Reaction in DMF/CH_2Br_2 (4 mL/1 mL). (g) Reaction in DMA/CH_2Cl_2 (4 mL/2 mL). (h) Reaction in DMF/$CHCl_3$ (1 mL/5 mL).

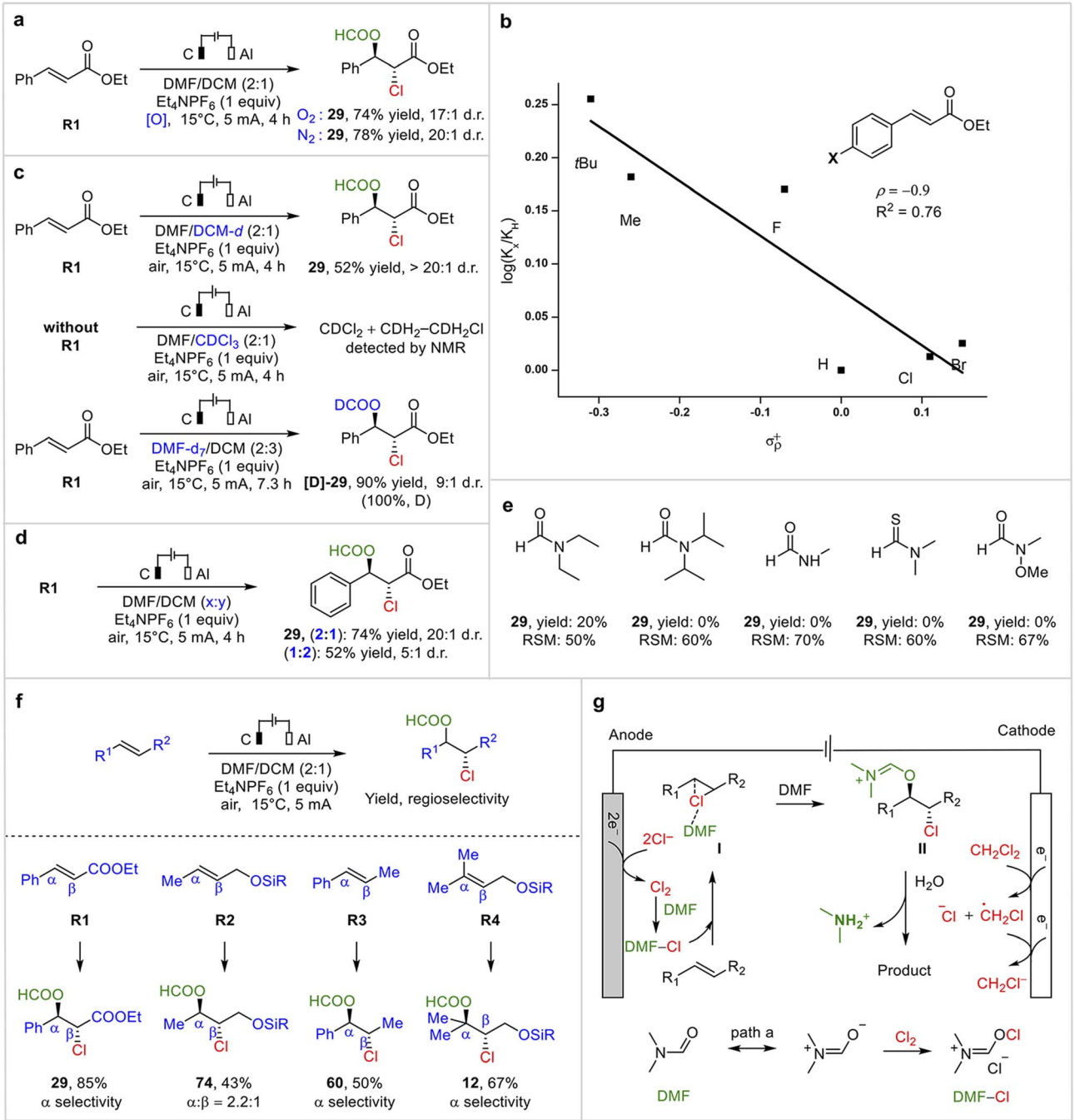

Scheme 4 Mechanism studies. (a) Radical trap experiments. (b) Hammett plot. (c) Deuterium experiments. (d) Stereoselective experiments. (e) Amide variant experiments. (f) Regioselective analyses of alkene haloesterification. (g) Proposed mechanism for modular intermolecular haloesterification. RSM, recovered start molecule. *R*, *tert*-butyldiphenyl.

a buildup of positive charge in the transition state of the rate-limiting step (Scheme 4b). This value aligned with the high site selectivity of this electrochemically electrophilic haloesterification in anti-addition across substrates with various electronic properties. An *R* value of 0.76 was obtained, indicating a moderately strong linear correlation, although the ideal value is ±1, suggesting that the reaction may be mainly controlled by electronic effects, with other contributing factors such as solvent participation, side reaction pathways or minor changes in the reaction mechanism (*e.g.*, transition from an S_E2 to an ion pair mechanism). A few deuterium experiments were also conducted (Scheme 4c). When using DCM-*d* instead of DCM, product **29** was obtained in a 52% yield, but product [D]-**29** was not detected. When the reaction was performed under standard conditions with DMF/$CDCl_3$ as the solvent but without alkene **R1**, NMR analysis of the crude reaction mixture detected $CDHCl_2$, indicating that $CDCl_3$ and DCM served as the Cl source *via* a consecutive paired-electrolysis-derived shuttle reaction.

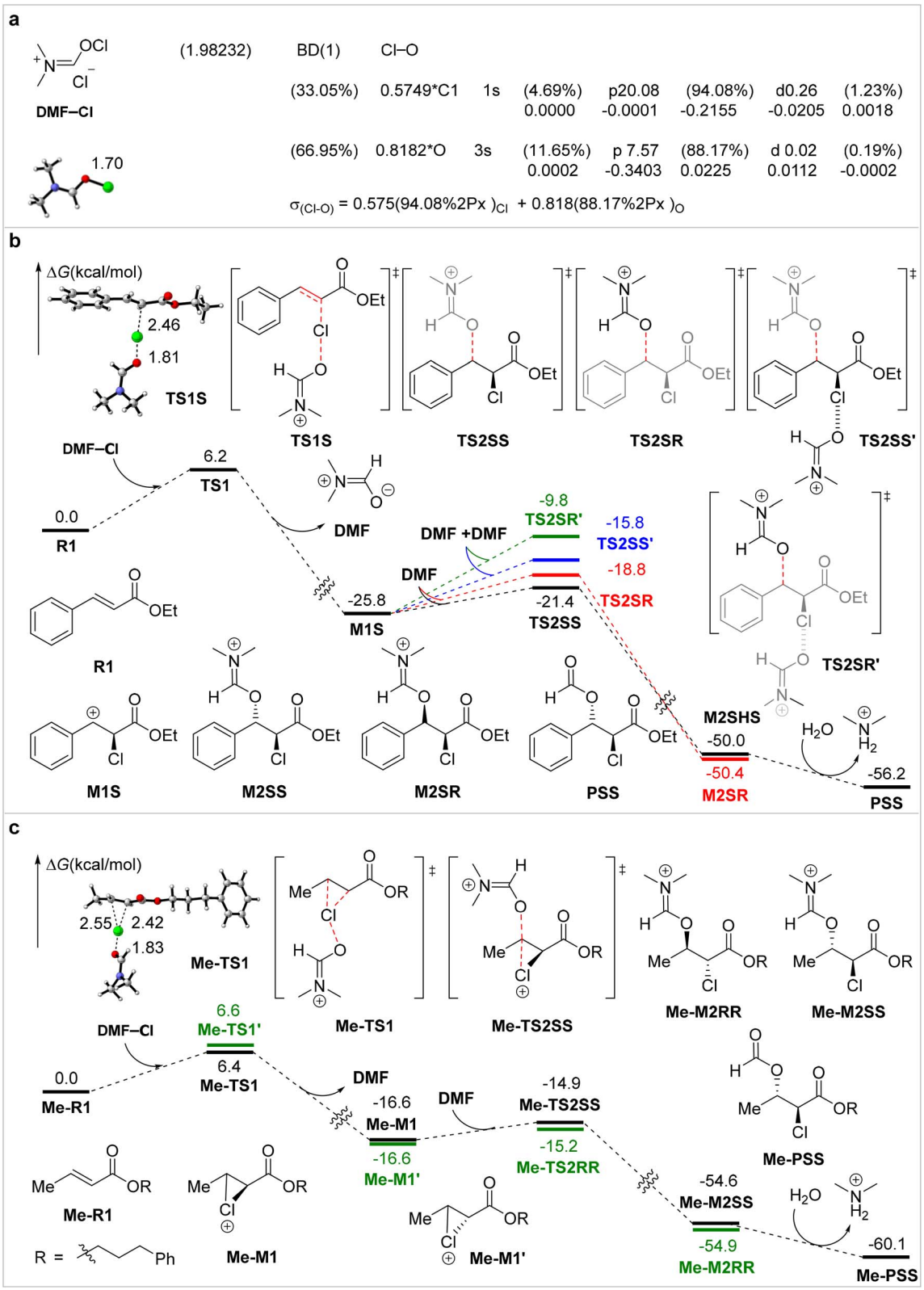

Scheme 5 DFT calculations for the proposed delivery mechanism and diastereoselectivity. (a) Nature orbital analysis for the Cl–O. (b) Gibbs free energy profile of DMF nucleophilic attack on phenyl-substituted substrate. (c) Gibbs free energy profile of DMF nucleophilic attack on methyl-substituted substrate.

Cyclic voltammetry studies clarified that X_2 was generated through sequential oxidation and reduction (Fig. S4–Al and S6). Upon replacing DMF with DMF-d_7, product [D]-**29** was obtained in a 78% yield with 100% D labeling, indicative of the aldehyde group of DMF participating in the haloesterification.

To further investigate the function of DMF, control experiments were carried out (Scheme 4d). They showed higher stereoselectivity with a higher relative amount of DMF. Furthermore, the reaction was found to be inhibited when increasing steric hindrance at the N atom of DMF, as well as when replacing one of the methyl groups with an H atom or an electron-deficient MeO group and replacing the O atom with an S atom (Scheme 4e). We propose that, in such reactions, DMF acts as a delivery reagent for halogen cations, promoting the selectivity of heterodifunctionalization in electron-deficient alkenes.

To determine the fundamental factors controlling regioselectivity, we focused on the nucleophilic attack of nucleophiles on the halogen-containing cation intermediate, with this attack considered to be the regioselectivity-determining step. The ability to stabilize the positive charge of the intermediate in internal alkenes was considered to be important, and as shown in Scheme 4f, we mutated the substituents of the alkenes to verify this hypothesis. For alkene **R1**, product **29** showed α-position selectivity and no β-position selectivity, aligning with the ability of the phenyl group to stabilize the positive charge. However, upon replacing the phenyl and ester groups with methyl and alkyl groups, respectively, at the α and β positions of alkene **R1** to afford electroneutral alkene **R2**, a significant decrease in α-position selectivity, with a regioselective ratio of $\alpha : \beta = 2.2 : 1$, was found. This result was attributed to the little difference between the electronic properties of the two carbons in alkene **R2**. Further substitution of the alkyl group with a phenyl ring in alkene **R2** to obtain alkene **R3**, or adding a methyl group at the α-position of alkene **R2** to yield the electroneutral trisubstituted alkene **R4**, enhanced α-position selectivity, due to the stability of the resultant cation species, arising from the π-conjugation effect of the phenyl ring or the hyperconjugation of the methyl groups. This result was indicative of the regioselectivity being governed by the stabilizing effects of substituents on the adduct cation, along with their electronic effects, with the position most capable of stabilizing the positive charge being involved in the determining step. An appropriate mechanism is shown in Scheme 4g. According to this mechanism, this electrolytic process begins with the cathodic reduction of DCM to produce Cl^-, which is then oxidized to Cl_2. The Cl_2 is captured by DMF to form DMF-Cl, which adds to the alkene to generate the halonium intermediate or β-halo carbocation **I**. The halo-containing intermediate **I** is then attacked by the nucleophilic oxygen variant of DMF, forming the imine intermediate **II**. Hydrolysis of this intermediate yields the desired haloesterification product. The consecutive-paired-electrolysis strategy for mediating the shuttle reaction of alkene heterodifunctionalization avoids the use of equivalent toxic, unstable, or low-reactivity halo reagents. Additionally, using DMF as a delivery reagent for halogen cations activates Cl_2 once it generates, and the reactivity and selectivity is enhanced, alkenes with high steric hindrance and low halenium affinity can achieve smooth haloesterification products, especially.

Density functional theory (DFT) calculations provided deeper insights into the halogen-cation delivery. Natural bond orbital analysis of Cl–O (Scheme 5a) suggested its σ-bond character, with the Cl–O bond length of 1.70 Å further indicating DMF-Cl to be the active species (which was also detected using HR-MS, Fig. S7–S10). The 3D structures of the transition states TS1S and Me-TS1, having phenyl- and alkyl-substituted electron-withdrawing substrates and DMF-Cl^+, shown in Schemes 5b and c, suggested a transport function of DMF between Cl^+ and the alkenes. The reaction mechanism and stereoselectivity were also clarified—with electrophilic attack by DMF-Cl on the phenyl-substituted substrate R1 generating the carbocation intermediate M1S, and subsequent nucleophilic attack proceeding through a transition state involving either a single DMF molecule or two DMF molecules. The Gibbs free energy difference between the two transition states, TS2SS and TS2SR (single DMF pathway), was calculated to be 2.6 kcal mol; a Boltzmann distribution analysis indicated this value to correspond to a 97% diastereomeric excess (de)—in good agreement with the experimentally observed diastereomeric ratio (dr > 20 : 1, de > 97%). Pathways involving two DMF molecules were also investigated, and the energy difference between transition states TS2SS′ and TS2SR′ was found to be 6.3 kcal mol^{-1}, corresponding to a calculated de value > 99%. Note the consistency of this exceptionally high selectivity with the experimentally determined dr > 20 : 1, supporting the finding that increasing DMF concentration can further enhance diastereoselectivity. For the reaction pathway involving the methyl-substituted substrate Me-R1, we have proposed a mechanism—involving electrophilic attack by DMF-Cl^+ to generate chloronium ion intermediates and subsequent S_N2 attack of these intermediates by DMF—that would account for the excellent anti-stereoselectivity observed in low-reactivity, electroneutral alkenes. To investigate the influence of DMF on the electrophilicity of the double-bond carbon atoms in the chloronium ion intermediates, Fukui function (f^+) analyses were performed for intermediates Me-M1, M3, M4, and M5, both in the presence and absence of DMF coordination (Fig. S11a). These analyses showed the presence of DMF having a minimal effect on f^+ for alkyl-substituted electron-withdrawing alkenes, but a more pronounced effect for electroneutral alkenes. Results of NBO charge calculations for alkene regioselectivity were found to be consistent with the experimentally observed regioselectivity (Fig. S11b).

Conclusions

In summary, we successfully achieved chemo-, regio-, and diastereoselective electrophilic haloesterification of both activated and unactivated alkenes, supported by an electrochemically oxidative 'electrophile–nucleophile' ('E–Nu') approach and promoted by a halogen-cation delivery mechanism. A wide range of alkenes are compatible with this strategy, yielding diverse vicinal haloesterification products with easily modifiable functional groups, in moderate to high yields,

regioselectivities and diastereoselectivities. It complements existing methods for the halofunctionalization of alkenes and marks a breakthrough in the construction of contiguous, multiple all-substituted carbon centers. The innovative methodology, in combination with consecutive paired electrolysis and halogen-cation delivery, realizes the electrophilic halofunctionalization of alkenes under mild and sustainable conditions, without the need for strong oxidants or highly corrosive halogenating reagents. This advancement enhances the feasibility of industrial and large-scale synthesis and provides technical support for catalytic asymmetric haloesterification of alkenes, especially electron-deficient and unactivated alkenes.

Author contributions

H.-H. X. conceived the project. H.-H. X., D. Q. and J. Z. performed the experiments and analyzed the data. H.-H. X., D. Q. and J. Z. contributed to the mechanistic studies. H.-H. X. Y. F. and H.-C. X. directed the project and wrote the manuscript.

Conflicts of interest

The authors declare no competing financial interests.

Data availability

CCDC 2481872 contains the supplementary crystallographic data for this paper.[43]

The data supporting this article are included in the supplementary information (SI). Supplementary information: experimental and syntheses procedures, characterisations including NMR, electrochemistry, spectroelectrochemistry, and DFT calculations. See DOI: https://doi.org/10.1039/d6sc00279j.

Acknowledgements

Financial support of this research from the National Natural Science Foundation of China (22001062, 52303350) and Henan Normal University are gratefully acknowledged.

References

1 C.-Z. Yao, X.-Q. Tu, H.-J. Jiang, Q. Li and J. Yu, *Tetrahedron Lett.*, 2023, **126**, 154639.
2 K. D. Ashtekar, A. Jaganathan, B. Borhan, D. C. Whitehead and S. E. Denmark, *Enantioselective Halofunctionalization of Alkenes in Organic Reactions*, 2021, pp. 1–266.
3 H. Mondal, *Chem. Eur J.*, 2024, **30**, e202402261.
4 A. Castellanos and S. P. Fletcher, *Chem. Eur J.*, 2011, **17**, 5766.
5 S. E. Denmark, W. E. Kuester and M. T. Burk, *Angew. Chem., Int. Ed.*, 2012, **51**, 10938.
6 U. Hennecke, *Chem.–Asian J.*, 2012, **7**, 456.
7 Y. Cai, X. Liu, P. Zhou and X. Feng, *J. Org. Chem.*, 2019, **84**, 1.
8 Y. A. Cheng, W. Z. Yu and Y. Y. Yeung, *Org. Biomol. Chem.*, 2014, **12**, 2333.
9 L. Zhou and J. Chen, *Synthesis*, 2014, **46**, 586.
10 J. Queder and G. Hilt, *Synlett*, 2024, **35**, 1906.
11 W. Zhang, N. Liu, C. M. Schienebeck, X. Zhou, I. I. Izhar, I. A. Guzei and W. Tang, *Chem. Sci.*, 2013, **4**, 2652.
12 C. Durgaiah, M. Naresh, M. Arun Kumar, P. Swamy, M. M. Reddy, K. Srujana and N. Narender, *Synth. Commun.*, 2016, **46**, 1133.
13 L. Li, C. Su, X. Liu, H. Tian and Y. Shi, *Org. Lett.*, 2014, **16**, 3728.
14 M. Naresh, P. Swamy, M. Arun Kumar, M. Mahender Reddy, K. Srujana and N. Narender, *Tetrahedron Lett.*, 2014, **55**, 3926.
15 I. Saikia, K. K. Rajbongshi and P. Phukan, *Tetrahedron Lett.*, 2012, **53**, 758.
16 L. Wang, H. Zhang, Q. Yu, C. Feng and J. Hu, *Synlett*, 2018, **29**, 1611.
17 T. Arai, K. Horigane, T. K. Suzuki, R. Itoh and M. Yamanaka, *Angew. Chem., Int. Ed.*, 2020, **59**, 12680.
18 F. Chen, X. Jiang, J. C. Er and Y.-Y. Yeung, *Tetrahedron Lett.*, 2010, **51**, 3433.
19 J. N. Kim, H. R. Kim and E. K. Ryu, *Synth. Commun.*, 1992, **22**, 2521.
20 C. Wan, R.-J. Song and J.-H. Li, *Org. Lett.*, 2019, **21**, 2800.
21 B. Soltanzadeh, A. Jaganathan, R. J. Staples and B. Borhan, *Angew. Chem., Int. Ed.*, 2015, **54**, 9517.
22 L. Liu, D. Zhang-Negrerie, Y. Du and K. Zhao, *Org. Lett.*, 2014, **16**, 436.
23 P. Pandit, K. S. Gayen, S. Khamarui, N. Chatterjee and D. K. Maiti, *Chem. Commun.*, 2011, **47**, 6933.
24 X. Sun, H.-X. Ma, T.-S. Mei, P. Fang and Y. Hu, *Org. Lett.*, 2019, **21**, 3167.
25 Y.-F. Tan, Y.-N. Zhao, D. Yang, J.-F. Lv, Z. Guan and Y.-H. He, *J. Org. Chem.*, 2023, **88**, 5161.
26 I. Micev, N. Christova, B. Panajotova and A. Jovtscheff, *Chem. Ber.*, 1973, **106**, 606.
27 J. S. Son, K. S. Jung, H. R. Kim and J. N. Kim, *Synth. Commun.*, 1998, **28**, 1847.
28 G. Hilt, *Chemelectrochem*, 2019, **7**, 395.
29 C. Ma, P. Fang, D. Liu, K. J. Jiao, P. S. Gao, H. Qiu and T. S. Mei, *Chem. Sci.*, 2021, **12**, 12866.
30 N. P. Martínez, M. Isaacs and K. K. Nanda, *New J. Chem.*, 2020, **44**, 5617.
31 N. Sbei, T. Hardwick and N. Ahmed, *ACS Sustain. Chem. Eng.*, 2021, **9**, 6148.
32 W. Zhang, N. Hong, L. Song and N. Fu, *Chem. Rec.*, 2021, **21**, 2574.
33 M. F. Hartmer and S. R. Waldvogel, *Chem. Commun.*, 2015, **51**, 16346.
34 D. Pollok and S. R. Waldvogel, *Chem. Sci.*, 2020, **11**, 12386.
35 X. Dong, J. L. Roeckl, S. R. Waldvogel and B. Morandi, *Science*, 2021, **371**, 507.
36 Y. Liang, F. Lin, Y. Adeli, R. Jin and N. Jiao, *Angew. Chem., Int. Ed.*, 2019, **58**, 4566.
37 X. Meng, Y. Zhang, J. Luo, F. Wang, X. Cao and S. Huang, *Org. Lett.*, 2020, **22**, 1169.
38 Z. Fu, F. Chen, G. Hao, X. Yi, J. Zeng and H. Cai, *Synthesis*, 2023, **55**, 3040.
39 T.-T. Zhang, M.-J. Luo, Y. Li, R.-J. Song and J.-H. Li, *Org. Lett.*, 2020, **22**, 7250.

40 X.-A. Liang, L. Niu, S. Wang and A. Lei, *Chem Catal.*, 2021, **1**, 1055.
41 K. D. Ashtekar, N. S. Marzijarani, A. Jaganathan, D. Holmes, J. E. Jackson and B. Borhan, *J. Am. Chem. Soc.*, 2014, **136**, 13355.
42 C. Hansch, A. Leo and R. W. Taft, *Chem. Rev.*, 1991, **91**, 165.
43 CCDC 2481872: Experimental Crystal Structure Determination, 2026, DOI: 10.5517/ccdc.csd.cc2p9ld0.